Non-Slice Selective Uniform Tipping RF Pulse Design for 3D MRI at High Field

H. Liu[1,2], and G. B. Matson[1,3]

[1]Center for Imaging of Neurodegenerative Diseases (CIND), Veterans Affairs Medical Center, San Francisco, CA, United States, [2]Northern California Institution for Research and Education, San Francisco, CA, United States, [3]University of California, San Francisco,CA, United States

Introduction

Overcoming the severe inhomogeneity of B_1^+ at high field (>3T) is a major challenge for providing uniform images. The non-uniform tipping produced by conventional RF pulses typically produces the well-known 'bright center' because of electrical properties of the imaged objects at higher field, which leads to spatially varying contrast and sub-optimal SNR, thus complicating interpretation and quantification of the images. Traditional methods to provide more uniform excitation include B_1 shimming (1), multi-dimensional RF pulse design (2,3), and new coil designs (4). For structural imaging, 3D sequences which do not use frequency-selective RF pulses have become popular. Recently, new pulse designs for non-slice-selective (NSS) pulses have been presented (5,6) which provide uniform tipping in the presence of inhomogeneous B_1^+ fields, and could potentially be used with such 3D sequences. We have also previously generated shallow tip angle NSS pulses using an optimal control optimization routine (7). In this study, we validated our shallow tip NSS RF pulse design through phantom tests and *in vivo* human studies, and further demonstrated that our methods also generate larger tip NSS pulses which are more efficient than previous designs (5,6). The advantages of these pulses for 3D MRI is that they can provide immunity to both B_1 inhomogeneity and resonance offset and can be applied with conventional head coils.

Methods

An optimization routine based on optimal control methods (8) was developed for NSS pulses and incorporated into MatPulse (9). The routine allowed the desired ranges of immunity to B_1 inhomogeneity and resonance offset to be specified, along with the maximum B_1 field (7). New designs of larger tips (30º, 60º, 90º and 180º) NSS RF pulses were generated and compared with recently published NSS pulses (5,6). The performance of a shallow tip design was verified experimentally on a silicon oil phantom, and advantages of the use of the shallow tip pulse were demonstrated with a 3D FLASH image on a human subject, using a TEM head coil at 4.0 T. Parameters for the FLASH image were: TR/TE = 5000 ms/1.45 ms, Inter-pulse delay = 100 ms, slices = 44, FOV = 300 mm.

Results and Discussion

Figure 1a shows a slice from a 3D FLASH image at 4T using a conventional 10º rectangular pulse, while Fig. 1b shows the signal intensity profile along the dotted line. Figure 2a shows the same slice from a 3D FLASH image using our NSS 10º pulse, while Fig. 2b shows the signal intensity profile along the dotted line at the same position as in Fig. 1a. The more uniform intensity and retention of contrast produced by the NSS pulse are evident.

As an example, the 90º NSS pulse produced in this work for Table 1 is shown in Fig. 3a. The performance of the pulse (in terms of transverse magnetization) shown in Fig. 3b as a contour plot, which demonstrates that this NSS pulse has B_1 immunity over more than ± 30% and over a range of resonance offset of ±250 Hz. The comparison of our larger tip angle NSS pulses with those of Moore et al (6) is shown in Table 1. The maximum B_1 field for the pulses was 15 uT, and the performance of the pulses is over the range of B_1 inhomogeneity and resonance offsets specified by Moore et al. (5), where the performance is specified by the average tip compared to the nominal tip, +/- the relative standard deviation of the tip (6). The power comparisons (P/Pblock) are the power required compared to a 15 uT rectangular pulse producing the same nominal tip (6). As shown, the NSS pulses produced in this work provided significant reductions in pulse length as compared to the Moore et al. pulses. Similar reductions in pulse length were estimated for the Boulant et al. (5) pulses. Experiments on a silicon oil phantom also verified our simulation of B_1 and off-resonance range immunities (Results not shown).
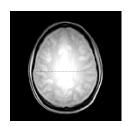

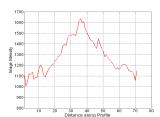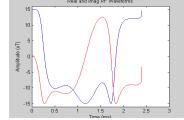Fig. 1a. 3D FLASH using a 10º rectangular pulse.
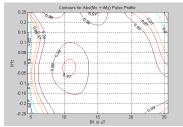

Fig. 1b. Intensity profile.

Fig. 3a. 90º NSS pulse (real and imaginary).

Fig. 3b. Contour plot of 90º NSS pulse performance.

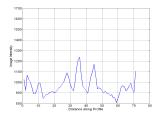Fig. 2a. 3D FLASH using a 10º NSS pulse.

Fig. 2b. Intensity profile.

Table 1. Comparison with Moore et al. Pulses

Tip	Pulse	Performance	Length(ms)	P/Pblock
30º	Moore et al.	0.98 +/- 0.07	4.10 ms	21.1
	This article	1.00 +/- 0.07	2.71 ms	19.8
60º	Moore et al.	0.98 +/- 0.08	4.10 ms	9.7
	This article	0.99 +/- 0.08	3.00 ms	9.4
90º	Moore et al.	0.97 +/- 0.10	4.10 ms	6.4
	This article	0.99 +/- 0.10	2.40 ms	6.1
180º	Moore et al.	0.92 +/- 0.10	4.10 ms	4.3
	This article.	0.91 +/- 0.09	3.20 ms	4.1

Conclusion

The removal of the bright center and rentention of image contrast due to the more uniform tipping were demonstrated by using our NSS RF pulse compared to conventional rectangular RF pulse. Table 1 demonstrated that the NSS pulses generated by MatPulse are shorter with similar or better performance than recently published NSS pulses (6). This study showed that our MatPulse optimization routine for NSS RF pulse designs can generate a full range of tips of non-slice-selective (NSS) RF pulses for 3D MRI with immunity to both B_1 inhomogeneity and resonance offset. While the advantage of uniform excitation is obvious (Fig. 1), Our NSS pulses do produce higher SAR (Table 1) and larger magnetization transfer effects (10) than the rectangular pulses they replace. Nevertheless, these pulses have the potential to generate uniform excitation of tissue at high magnetic field. The MatPulse program is available from www.cind.research.va.gov. This work was supported by NIH grants 5R01EB000766 and 1P41RR023953.

References: [1] Mao W et al. MRM 56, 918, 2006. [2] Katscher U et al. MRM 49, 144, 2003. [3] Zhu Y et al. MRM 51, 775, 2004 [4] Wang et al IEEE Trans Med Imaging 28, 551, 2009. [5] Boulant N et al. MRM 61, 165, 2009. [6] Moore JE et al. J Magn Reson 205, 50, 2010. [7] Matson GB et al. J Magn Reson 199, 30, 2009. [8] Skinner et al. J Magn. Reson. 1671, 68, 2004. [9] Matson GB. Magn Reson Imaging 12, 1205, 1994. [10] Matson et al. ISMRM 18 (2010), Prog# 3008. .